Chapter 1
A comprehensive study of hydrogen redistribution and embrittlement prevention in ferrous alloys

Daniel GAUDE-FUGAROLAS

Abstract Hydrogen may cause severe degradation on some high strength alloys, and due to their technological and economic relevance, research efforts have intensified in recent years to improve our understanding of such phenomena. A physical model of interstitial element diffusion has been used to study the fluxes of hydrogen during manufacturing of metallic alloys. In particular, the present model contemplates diffusion in its most comprehensive description, i.e., atom diffusion is driven by the gradient in chemical activation, instead of simply occurring down the composition gradients. The model incorporates as well the influence of thermal history, microstructure, matrix solubility, multiple trapping distributions, and interaction with the atmosphere. This model is able to describe and predict the behaviour of hydrogen during standard industrial practices, and it has been used to explain the effect of component size, cooling rate, microstructure, deformation level, dislocation distribution, grain size, carbide presence and distribution, phase transformation temperature, baking conditions, et c. on hydrogen redistribution. Furthermore, by estimating possible supersaturation at specific regions in the component, it allows to anticipate defect formation and embrittlement risk (and therefore, to prevent them). Not only that, but by using this model, a method has been developed which enables to reduce hydrogen content from the metal via the use of imposed temperature gradients. This method has recently obtained several patents.

Daniel GAUDE-FUGAROLAS
dgaude Prime Innovation SLU
c/. Alcalde Joan Batalla, 4,
08340 Vilassar de Mar (Spain)
e-mail: dgaude@cantab.net

1.1 Introduction

Hydrogen is well known to cause severe degradation on high performance alloys [24, 3, 28, 6]. Because of the economical, technological and safety repercusions, this phenomenon has attracted intense interest for long time [22, 25, 26].

Alloy embrittlement is influenced by the way hydrogen redistributes and the sites where it becomes trapped. Understanding the redistribution of hydrogen correctly would allow to predict and, if necessary, prevent this type of material degradation.

The work presented here describes the development of a physical model on interstitial diffusion and its application towards the study of hydrogen redistribution patterns during various metallurgical processes, like casting and various heat treatments. By understanding the behaviour of hydrogen in the metal, it is possible to predict when, where and what type of damage might occur. Finally, during this research project a new method has been developed for the extraction of hydrogen from metal alloys [16, 18, 11].

1.2 Description of the model

A physical model describing the diffusion of interstitial atoms has been developed and used to study the redistribution of hydrogen [14, 16]. Phase transformations during any treatment are modelled using thermodynamic criteria and classic nucleation and growth kinetics as described in previous work [12, 13].

1.2.1 Hydrogen diffusion

In a rigorous definition of diffusion, its driving force is related to the gradient of chemical potential (and not just to the composition gradient, as often seen in simpler approximations) [7]. Thus, as long as we assume dilute solution of the interstitial elements, the gradient in chemical potential of an interstitial atom is related to the gradient in partial saturation at the matrix phase [22, 25, 2]. Consequently, the actual flux of atoms becomes a function of the relative saturation, that is, interstitial atoms will tend to flow from regions with high levels of saturation to regions with lower levels of saturation (*i.e.* down-hill the partial saturation gradient). For instance, in the case of uniform temperature this would lead to atoms flowing from regions with high concentration to regions with low concentration, but in a system with large temperature (and therefore solubility) gradients, or with phases with distinct solubilities, a correct diffusion description allows other possibilities, like diffusion happening up-hill the composition gradient [7, 14, 16].

Hydrogen distribution evolution is determined from thermal agitation and atom mobility by relating it to a random walk process. The distance covered by each atom,

the mean random walk distance, Δx, in a time interval t, is related to the thermal agitation, via the diffusion coefficient D, using the random walk expression [1]:

$$\Delta x = \sqrt{\Delta t \cdot D} \tag{1.1}$$

The effect of thermal activation is captured by an Arrhenius-type description of diffusion, with the diffusion pre-exponential and activation energy coefficients obtained from literature [26, 27, 8, 9].

If each atom jump were totally random, the probability, P, of an atom ending its random walk in the adjoining cell in direction j would be given by,

$$P = \frac{1}{6}\frac{\Delta x}{l_c} \tag{1.2}$$

where l_c is the calculation cell length in one of the 6 main directions of displacement. In the model these probabilities are then modified to account for the gradients in partial saturation.

The differences in partial saturation in adjoining regions are used to determine the probability of atoms diffusing. Additionally, the issue of site saturation is also dealt with by considering partial saturation [16].

1.2.2 Supersaturation and equivalent gas pressure

The alloy's microstructure is only able to store a small amount of hydrogen between the lattice and various types of lattice defects. In some cases, these defects consist in subtle distortions of the lattice itself, like the distortion around dislocations, or on the surfaces of a coherent precipitates. Othertimes, defects represent a severe rupture of the lattice structure, like for instance voids, microcracks or the surfaces of specific incoherent precipitates.

The resulting effect on the mechanical properties of the alloy depends directly on the type of trapping site and the amount of hydrogen that contains. As several types of trapping sites coexist, different and competing embrittlement mechanisms might be at work simultaneously [22].

In microcracks for instance, hydrogen trapped in large concentrations may transform into its molecular form (gas), and produce an increase in pressure inside the defect, potentially leading to irreversible damage in the form of cracking and plastic deformation (fisheyes, flaking, etc.) [31, 22].

An illustrative parameter to estimate the risk of hydrogen embrittlement is the equivalent gas pressure in a microcavity due to supersaturation. Besides, even though the physical meaning of the equivalent gas pressure becomes less clear for trapping sites other than microcavities, it is still a good parameter of the embrittlement risk from superaturation. Therefore, this equivalemt gas pressure is calculated for each the lattice and all trapping sites considered, not necessarily as a physical

prediction of actual pressure, but as a convenient estimate of the potential embrittlement risk, as described elsewhere [15].

Nevertheless, section 1.2.5 goes one step further, using this pressure parameter for a physically meaningful estimation of embrittlement risk, accounting for the effect of evolving mechanical properties, microstructure and defect distribution.

1.2.3 Trapping

The model describes the redistribution of hydrogen into various types of trap assuming that any hydrogen contained in the metal either stays in solution up to the lattice phase's solubility limit or it is expelled from the lattice and becomes *trapped* into various types of lattice defects available. Also, a diffusing hydrogen atom may become trapped as it comes across with lattice defects while partitioning [17, 8, 9].
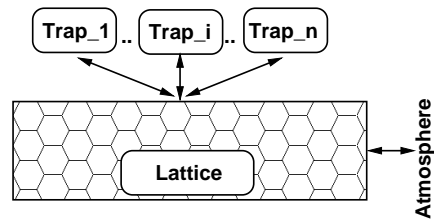

Fig. 1.1 Hydrogen redistribution fluxes between the atmosphere, the lattice and n trap site types.

The nature of trapping sites vary, but they can all be described as a potential well, in the same way as lattice diffusion sites. Each trap type is then characterised by the specific activation energy, E_t, necessary for the release of an hydrogen atom contained in them[22, 17]

1.2.4 Hydrogen desorption

To consider free surfaces and their effect on the behaviour of interstitial atoms, specially those as mobile as hydrogen, hydrogen desorption is estimated assuming local equilibrium at the surface. Then, the relationship between hydrogen dissolved in the metal at the surface and the partial pressure of hydrogen gas in the atmosphere follows Sievert's law [22, 25, 27]. Additionally, the flux of hydrogen atoms across the surface is still restricted by the atom mobility conditions and by site saturation (*i.e.* partial saturation), as described earlier [15, 16].

1.2.5 Prediction of permanent hydrogen damage

Hydrogen embrittlement is a complex phenomenon with multiple and often competing mechanisms, including HIE (Hydride-induced embrittlement), AIDE (Adsorption-induced dislocation-emission), HELP (Hydrogen enhanced localised plasticity), HEDE (Hydrogen enhanced decohesion mechanism) and others [20, 4].

However, having a set of criteria able to predict the threshold of permanent damage in real structural components and during industrial practices would perform an invaluable service during component manufacturing and process supervision.

Permanent damage in a ductile materials occur when the capacity of elastic (*i.e.* reversible) deformation is exceeded and plastic (*i.e.* irreversible) deformation develops. Brittle fracture, on the other hand, takes place when the energy required to create fresh fracture surfaces is lower that the energy to activate any of the available deformation mechanisms able to reduce the stress distribution by yielding under the stress [4, 20]. In the first case, and for commercial ferrous alloys, the onset of plastic deformation happens around the point where shear stress τ reach $10^{-3} \cdot G$, where G is the Shear Modulus of the metal for that alloy composition, phase and temperature [10]. In engineering terms it is usually expressed as 0.1% of shear deformation ($\gamma = \tau / G = 0.001$) [4].

As described previously, hydrogen supersaturation could be represented as a stress distribution equivalent to an hydrostatic pressure on the lattice structure, akin to the real pressure within existing micro-defects like micro-cracks, voids and incoherent interfaces [15]. By determining the equivalent pressure in the lattice and then applying the criterion described above, it is possible to estimate the risk of irreversible deformation and therefore, the onset of permanent damage in the metal component [19].

1.3 Results and discussion

Using this model the influence of manufacturing parameters and material conditions on the redistribution of hydrogen in steel have been studied. Starting with a description of the hydrogen redistribution occurring during a cooling process, then a detailed study of *baking*, a commonly used method against of hydrogen embrittlement. The prediction of permanent damage in the alloy has also been analysed, paying special attention to the effect of mechanical properties, microstucture and defect distribution. Most importantly, the improved understanding of hydrogen redistribution has allowed to design a novel method for the reduction of hydrogen content in metallic alloys, with the aim to reduce the risk of hydrogen embrittlement at a lower cost.

1.3.1 Description of cooling

A generic cooling process has been studied with the model described above, in order to obtain a better understanding of the effect of process parameters to the redistribution of hydrogen [16]. This simulation could be applied to casting, for instance, or any other cooling process.

An aspect of interstitial redistribution that often is not well understood is the effect of cooling rate. Fig.1.2 presents the different hydrogen distribution obtained with either a fast or a slow cooling processes applied to a steel plate 25cm thick and containing 2ppm of hydrogen. These calculations show how during a long and slow cooling ($h = 6Wm^{-2}K^{-1}$), and while the surface is still at high temperature, a portion of hydrogen diffuses away from the subsurface region and out into the surrounding atmosphere, and as the temperature gradients within decrease the hydrogen concentration homogenises to an average content of 1.53ppm.

Conversely, during an accelerated cooling ($h = 22 \cdot 10^3 Wm^{-2}K^{-1}$), the large temperature gradient between the surface and the core of the component encourage the hydrogen flux towards the core region. Simultaneously, as the surface temperature decreases rapidly, desorption to the atmosphere is reduced. Additionally, as the metal cools and undergoes phase transformation from FCC to BCC, the flux towards the core region is favoured as the later phase is less able to dissolve hydrogen.
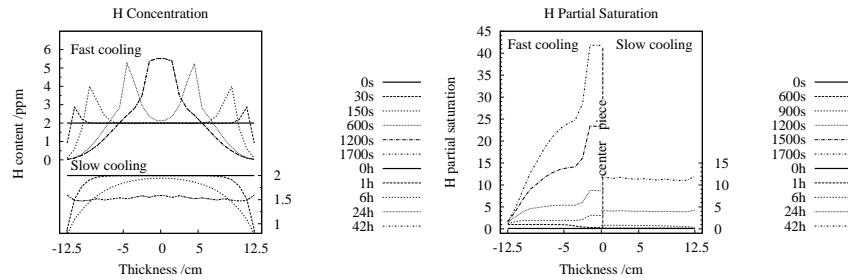

Fig. 1.2 Hydrogen redistribution during fast and slow cooling of a 25cm thick plate with 2ppm start H content. Concentration and partial saturation (or supersaturation if above 1.0).

During a long and slow cooling, hydrogen content remains homogeneously distributed, and although hydrogen content reaches supersaturation and increases to several times the solubility of the BCC matrix, the supersaturation is still substantially less severe than in the core region of a fast cooled component. For the example presented here, the fast cooled component starting with a hydrogen content of 2.0ppm reaches in its core region supersaturation over 40 times the solubility limit of the BCC matrix.

Component size intensifies this effect, as a larger volume implies larger absolute hydrogen content for the same average content. The FCC to BCC transformation

temperature, also influence the intensity of this redistribution. Both effects are presented in Fig. 1.3 [16].
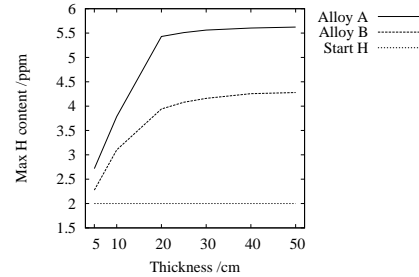
Fig. 1.3 Effect of component size and FCC/BCC phase transformation temperature on hydrogen concentration after fast cooling. Steel A transfroms at 700°C and Steel B at 450°C.

1.3.2 Description of baking

Baking is a method used commonly to minimise the detrimental effect of hydrogen on the mechanical properties of a metal component. Typically, this type of treatment consists in storing the metal component at *low* temperature (*i.e.* 150 to 230°C) for a long period of time (typically 12 to 48 hours) [5].

The aim of the treatment is that a fraction of the hydrogen in the lattice diffuses to the surface of the component from where it escapes to the atmosphere. However, and as clearly described by the simulations, the picture is more complex. On one hand, a quantity of hydrogen becomes stored also in microstructure defects, or *traps*. Hydrogen atoms in such *trap* sites need to overcome the detrapping energy barrier characteristic to the type of site, while at the low temperature of the treatment, this is not always possible [30, 29, 23, 18]. On the other hand, saturation of the lattice impedes the diffusion of hydrogen atoms.

To analyse which parameters affect the effectiveness of baking, two steel microstructures have been considered, defined by the temperature of transition from FCC to BCC during cooling and their characteristic microstructures. The microstructures are described in terms of characteristic dislocation density and grain size but whose carbide distributions are similar (Table 1.1). These parameters define both the trap density and distribution, each trap defined by its energy barrier [17, 18].

For this simulation, the starting hydrogen distribution in the metal is defined by the temperature cycle prior to the baking treatment. For this example it consists in a continuous cooling from 1600°C to room temperature, immediatelly followed by a 12 hour baking treatment. Two baking temperatures have been considered for the simulation (190°C and 300°C).
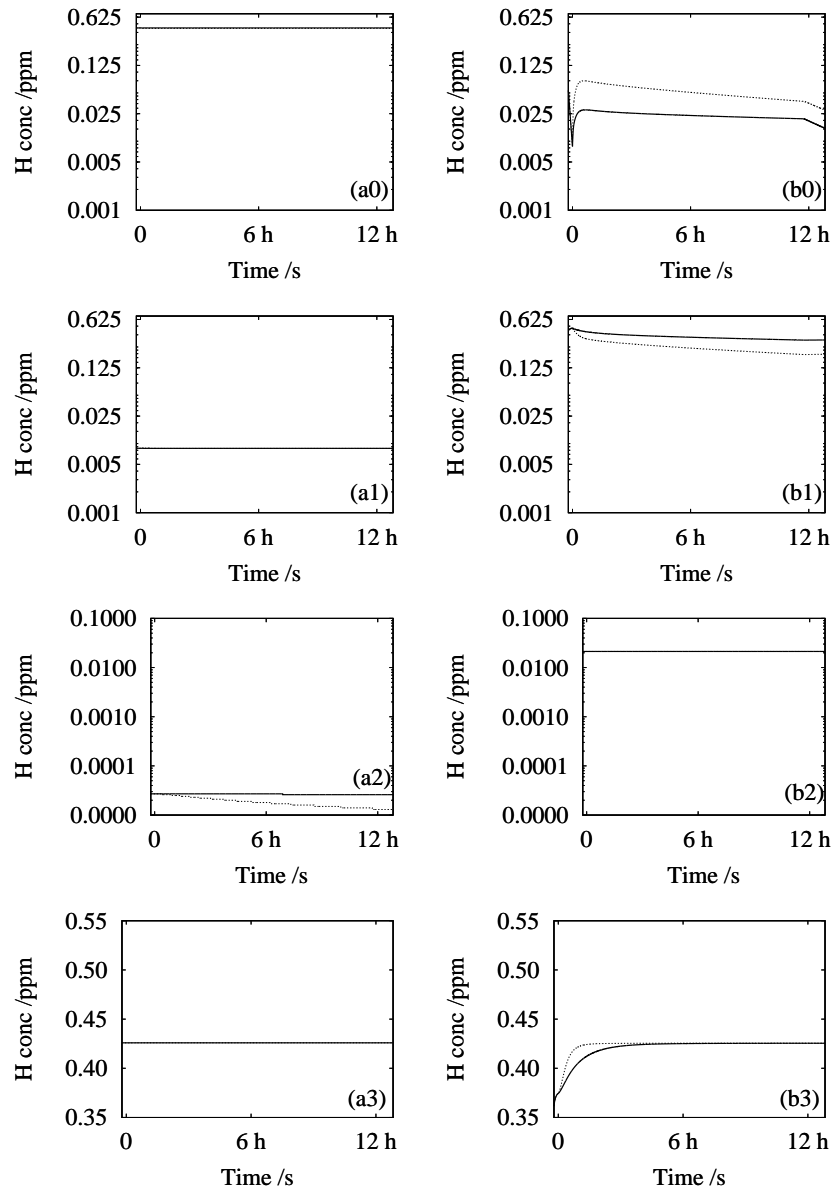
Fig. 1.4 Hydrogen redistribution curves during baking for two microstructures and two baking temperatures, detailing the hydrogern content evolution for lattice and each type of trap sites. **ax)** and **bx)** refer to Steels A and B, indexes **0** to **3** to lattice, dislocation, grain boundary and precipitate trapping sites respectively. Solid line correspond to baking temperature of 190°C and dotted line to 300°C.

Table 1.1 Austenite decomposition temperature and final microstructure obtained from its decomposition, and trapping site distribution for Steel A and Steel B.

	Steel A	Steel B
FCC → BCC:	725°C	450°C
BCC Microstructure:	Allotriomorphic Ferrite	Acicular Ferrite
Grain size:	Large 0.1 mm	Small 10μm
Dislocation site density:	Low $4\cdot10^{22}site/m^{3}$	High $4\cdot10^{24}site/m^{3}$
Ppt. trap site density:	$2\cdot10^{22}site/m^{3}$	$2\cdot10^{22}site/m^{3}$

Fig.1.4 shows how the overall hydrogen content, microstructure and trap distribution interact in a complex way during any thermal treatment, as in this case in a baking treatment [18].

The capacity of hydrogen to diffuse is, *a grosso modo*, inversely dependent on the degree of saturation of the lattice. Therefore, any baking treatment will be more effective when applied to an alloy presenting a microstructure better suited to absorb large concentrations of hydrogen before becoming saturated than on an alloy that is already saturated at the start of the treatment.

The hydrogen reduction obtained for both microstructures and baking temperatures is presented in table 1.2. An alloy with smaller grain size, larger dislocation densitiy and more extensive precipitate or inclusion distribution will have a larger capacity to absorb hydrogen before becoming saturated. Therefore, an acicular or bainitic ferrite microstructure for instance, containing large dislocation network combined with a fine precipitate distribution will tolerate dissolving more hydrogen before becoming saturated, and therefore it will also be more effective at discarding it during a baking treatment than another microstructure with, for instance, large grained allotriomorphic ferrite, low dislocation density and few carbide surface area.

Table 1.2 Reduction in hydrogen content during baking for 12 h at 190°C and 300°C for Steel A and Steel B.

Baking T	Steel A	Steel B
190°C	0.005%	9.2%
300°C	0.6%	19.6%

The role played by different types of traps is first, function of their partial saturation related to the lattice and second, of their characteristic energy barrier to the release of hydrogen. While the lattice presents lower partial saturation and the temperature allows the release of hydrogen from the trap distribution, the flux of

hydrogen will occur towards the lattice (and eventually to the atmosphere). However, for traps with a large energy barrier (*deep traps*) it is possible that they keep absorbing hydrogen while the rest of the microstructure releases hydrogen to the atmosphere [18].

1.3.3 Design of hydrogen extraction method

The deeper understanding of the fluxes of hydrogen in metals obtained using the model described above has allowed to design a novel method to eliminate hydrogen from metallic alloys [16, 11].

As already discussed in section 1.3.1, during the process of cooling a component the flux of hydrogen occurs towards the core of the metal component, because it stays at higher temperature as heat is extracted from all the surface of the component. However, if we consider a case where a small region of the surface of that component were to be kept at high temperature during the cooling process, hydrogen would still flow towards the hot regions of the component, with the difference that in this case, it would not accumulate in the core region but under the heated surface from where it would eventually diffuse to the atmosphere, as illustrated in Fig.1.5 [16, 11].
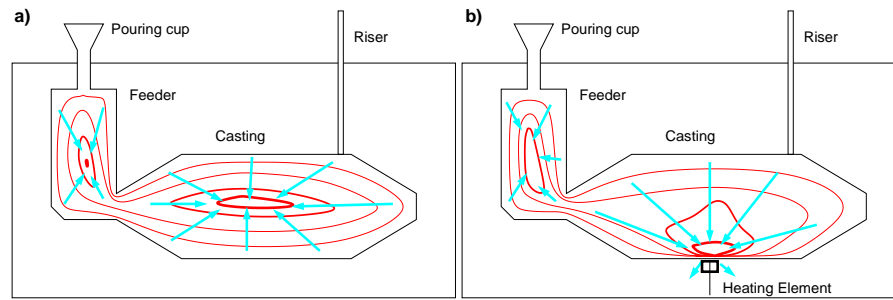

Fig. 1.5 a) Schematic of hydrogen redistribution during a standard casting process. b) Modiffied hydrogen redistribution when diffusion fluxes are redirected to a heated region at the surface.

The evolution of hydrogen distribution during such an operation is summarised in Fig.1.6. A 25cm thick plate, as in the calculation in Section 1.3.1, is cooled from 1600^oC to just above room temperature. However, in this case while one face of the plate is severely cooled ($h = 22 \cdot 10^3 Wm^{-2}K^{-1}$) the one opposite is kept at 1500^oC for 7200s. (2 hour). During this process the overall hydrogen content decreases to less than half the starting content (*i.e.* from 2ppm to 0.99ppm).

During the treatment a severe concentration peak still occurs. However, on this case it occurs only while the material is at high temperature and it is able to dissolve the large interstitial content. Fig 1.6 illustrates how the partial saturation remains below saturation during all the treatment, only increasing slightly during cooling to
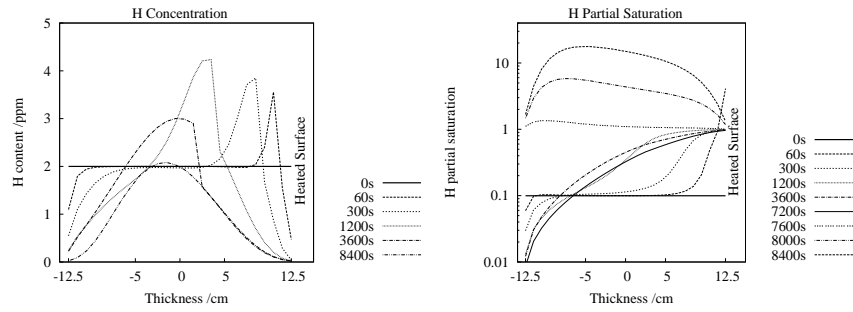
Fig. 1.6 Hydrogen redistribution during directional cooling of a 25cm thick steel plate, where one of its surfaces is kept at 1500°C for 7200s. Concentration and partial saturation (or supersaturation if above 1.0).

room temperature after the treatment. Even then, the final supersaturation is similar to what would result of an extremely slow cooling.

While the treatment proceeds hydrogen is released to the atmosphere through the heated region, and the overall content and the magnitude of the concentration peak both decrease. At the end of the treatment the overall hydrogen content has been halved, to reach 0.99ppm. This is sensibly lower than the 1.53ppm obtained during extremely slow cooling, and taking only 8400s (2 hours and 20 minutes) instead of 42 hours by slow cooling or over 12h by baking.

Furthermore, by taking into account the geometry of the component and the hydrogen content requirements and with tools like the model presented here, it is possible to design tailored heat treatments optimising the final hydrogen content and distribution, and even limiting the maximum concentration peaks by adjusting parameters like the temperature of treatment and severity of cooling.

1.3.4 Prediction of permanent hydrogen damage

Most industrial alloys are polycrystalline and often multiphase. The availability of deformation mechanisms able to reduce an applied stress vary with metallographic orientation in the grain, and this varies from grain to grain. Therefore, any internal stress distribution will also depend to a certain extent on the grain orientation distribution. For this reason, any criteria on the onset of permanent damage in the metal necessarily can only be approximate, and a margin of safety needs to be considered. Nevertheless, the development of criteria predicting the inception of permanent damage in structural components is invaluable in component production and process design and supervision.

1.3.4.1 Simulations used

This section presents calculations of hydrogen redistribution on a large component (1.5m in thickness) during solidification and constant cooling to room temperature (with h = 2000 $Wm^{-2}K^{-1}$). Two different alloys have been simulated: *Steel A* with FCC to BCC transformation at 725°C producing ferrite characterised by larger grain size (100 μm) and an intermediate dislocation density (10^{12} m^{-2}), and *Steel B* with FCC to BCC transformation at 450°C producing ferrite characterised by smaller grain size (10 μm) and high dislocation density (10^{14} m^{-2}). The starting hydrogen content levels considered are 1.0 and 3.5 ppm.

1.3.4.2 Lattice hydrogen supersaturation and microplasticity damage
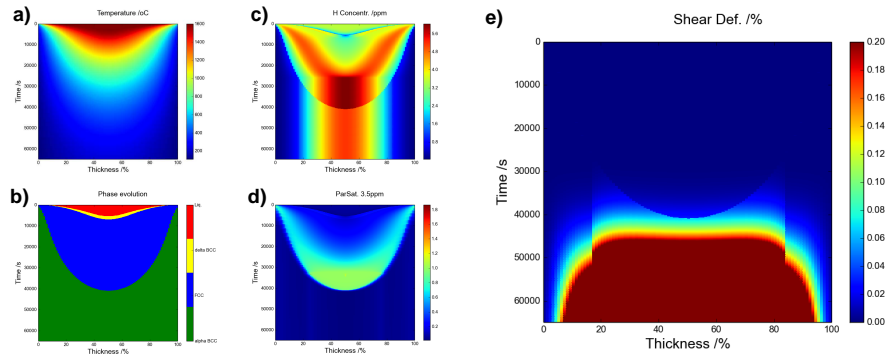

Fig. 1.7 Plots presenting the evolution of a) temperature, b) phase, c) hydrogen concentration, d) hydrogen partial saturation in the metal lattice and e) shear deformation (as criteria for micro-damage risk) during solidification and cooling of a 1.5 m thick steel component with a homogeneous starting hydrogen concentration of 3.5 ppm. FCC to BCC phase transformation occurring at 450°C.

Fig. 1.7 illustrates the application of the criterion described in section1.2.5. A component made with alloy *Steel B* and containing 3.5 ppm of hydrogen solidifies and is actively cooled to room temperature. The evolution of temperature as well as the phase evolution during cooling and at any position within the thickness of the component are shown respectively in Fig. 1.7 a) and b). During this cooling process hydrogen redistributes, and different regions in the ferritic lattice attain a range of hydrogen partial saturation levels or in some regions even supersaturation. By determining the equivalent hydrogen gas pressure related to those regions where supersaturation occurs, and then applying the criterion of $\tau = 10^{-3} \cdot$G, (with *G* the Shear Modulus of the metal) it is possible to estimate the risk of permanent damage to the component due to microplasticity. $\tau = 10^{-3} \cdot$G is equivalent to shear deformation $\gamma = 0.1\%$ [19, 4].

In this example it is observed the apparition, just before 30 ks, of two regions around 20% and 80% of the thickness of the component where the shear strain starts to build up towards the yield shear strain limit defined above. As the process progresses, at around 45 ks, these two regions converge into a larger region comprising the whole core of the component. Within this region strain levels reach values considered to be unsustainable.

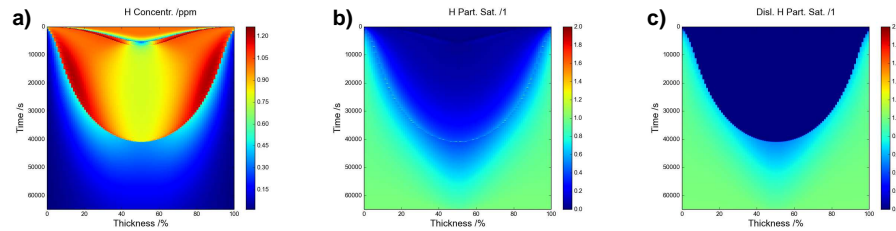### 1.3.4.3 Hydrogen saturation in dislocation distribution

Fig. 1.8 Plots presenting a) the evolution of hydrogen concentration in metal lattice, b) hydrogen partial saturation in lattice and c) hydrogen partial saturation in dislocation distribution, during solidification and cooling of a 1.5 m thick steel component with a homogeneous starting hydrogen concentration of 1.0 ppm. Temperature and phase evolution identical to those shown in Fig 1.7 a) and b). FCC to BCC phase transformation occurring at 450°C.

Another criterion proposed here to estimate the risk of embrittlement of an alloy under the influence of hydrogen consists in observing the degree of partial saturation of the dislocation distribution [19]. A dislocation distribution presenting a large partial saturations in hydrogen is expected to behave differently than when free of hydrogen presence [4, 21].

Fig. 1.8 illustrates the calculations for a component of the same alloy and geometry as in the example above (section 1.3.4.2) but containing only 1.0 ppm of hydrogen. The evolution of temperature as well as the phase evolution during cooling are identical as shown in Fig. 1.7 a) and b).

In this example, lattice partial saturation stays close to saturation but never reaching severe supersaturation, and therefore (by applying the microplasticity criterion above) without expected risk of embrittlement due to that mechanism. On the other hand, the dislocation distribution in the ferrite phase also becomes close to saturation. It is at this moment that needs to be pondered what could be the effect of a hydrogen saturated dislocation distribution. If dislocations become blocked due to hydrogen then the metal would be expected to develop hardening and decreased ductility, eventually producing embrittlement of the material. At the same time, the severity of this effect is ultimately related to the ability of the alloy to create new dislocations and therefore accommodate new deformation [19].

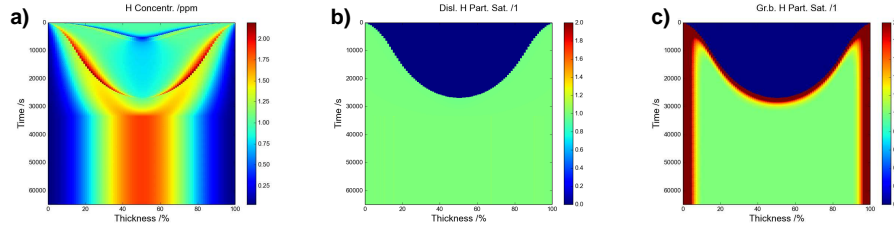### 1.3.4.4 Hydrogen saturation at grain boundaries

Fig. 1.9 Plots presenting the a) evolution of hydrogen concentration in metal lattice, b) hydrogen partial saturation in dislocation distribution, and c) hydrogen partial saturation at grain boundaries during solidification and cooling of a 1.5 m thick steel component with a homogeneous starting hydrogen concentration of 1.0 ppm. Temperature evolution identical to that shown in Fig 1.7 a). FCC to BCC transformation occurring instead at 725°C.

The last criterion proposed in this work for the estimation of the embrittlement risk of an alloy under the influence of hydrogen is based on determining the hydrogen partial saturation at grain boundaries (and similarly for precipitate interfaces) [19]. A grain boundary with hydrogen supersaturation could become embrittled due to various mechanisms, ranging from the obstruction of the deformation mechanisms characteristic of grain boundaries, to the apparition of microplasticity damage similar to what is described in section 1.3.4.2 for the metal lattice[20].

Fig. 1.9 illustrates the calculations for a component of the same geometry as in the examples above (section 1.3.4.2), but in a different alloy, *Steel A*. In *Steel A* austenite transforms to ferrite at higher temperature than in *Steel B* and with different characteristics (larger grain, lower dislocation density). For this calculation, the steel contains only 1.0 ppm of hydrogen. The evolution of temperature is identical as for other examples in this work, and already shown in Fig. 1.7 a).

Steel A's microstructure is less able to dissolve hydrogen in its trap site distribution than *Steel B* of earlier examples (sections 1.3.4.2 and 1.3.4.3). In this case, the hydrogen dissolved in the lattice tends to concentrates at the core of the component, while the dislocation distribution become immediately saturated after transformation from austenite to ferrite. The interesting aspect though is the distribution of hydrogen at the grain boundary trapping sites. Actually, grain boundaries become severely supersaturated on transformation to ferrite. As the process proceeds, hydrogen in grain boundaries at a distance from the surface redistributes elsewhere reducing grain boundary supersaturation to levels close to full saturation. Grain boundaries close to the surface however, where the temperature does not allow sufficient redistribution of hydrogen, remain supersaturated till the end of the process (Fig. 1.9 c)). In both cases, the degree of supersaturation would suggest a risk of embrittlement. In particular, for the surface grain boundaries, this could explain various be a mechanisms of intergranular brittle fracture and crack formation in the surface and immediate subsurface regions.

1.4 Conclusions

A model on hydrogen diffusion had been presented able to describe accurately hydrogen redistribution during manufacturing processes.

Using this model it is possible to describe and predict the behaviour of hydrogen during standard industrial practices, and it has been used to explain the individual effects of parameters like component size, cooling rate, microstructure, and phase transformation temperature on hydrogen redistribution.

Furthermore, it permits to explain in which circumstances and to what extent a baking treatment would be effective at reducing hydrogen from a component and when it would not, and to relate that to process parameters like hydrogen content, steel microstructure and treatment parameters.

The model is also able to predict, based on physical criteria, the risk of hydrogen damage based on the fact that severe supersaturation of either lattice or any defect structures in the metal is involved in damage formation and embrittlement of the metal. For this, three criteria have been presented for the prediction different embrittlement mechanisms:

- A microplasticity threshold related to *Shear Modulus* as predictor to lattice microcracking.
- Dislocation supersaturation as a possible origin for ductility loss.
- Grain boundary supersaturation as a possible origin for intergranular decohesion, as well as of subsurface defects like *flaking*.

Last but not least, during the course of this work a method has been developed to reduce hydrogen content from the metal via the use of imposed temperature gradients. This method has recently obtained several patents [11].

References

1. Ågren, J.: Numerical treatment of diffusional reactions in multicomponent alloys. Journal of Physics and Chemistry of Solids **43**, 385–391 (1982)
2. Bockris, J.O., Beck, W., Genshaw, M.A., Subramanyan, P.K., Williams, F.S.: The effect of stress on the chemical potential of hydrogen in iron and steel. Acta Metallurgica **19**, 1209–1218 (1971)
3. Clayton, C.Y., Foley, F.B., Laney, F.B.: Flaky and woody fractures in nickel-steel gun forgings. Transactions of the Metallurgical Society of AIME **62**, 211–245 (1919)
4. Cottrell, A.: An introduction to metallurgy. The Institute of Materials, London (1995)
5. Cramer, S.D., Covino, B.S.J.: ASM Metals Handbook 13A – Corrosion Fundamentals, Testing and Protection. ASM, US (2003)
6. Dana Jr., A.W., Shortsleeve, F.J., Troiano, A.R.: Relation of flake formation in steel to hydrogen, microstructure, and stress. Journal of Metals – Transactions AIME **203**, 895–905 (1955)
7. Darken, L.S., Oriani, R.A.: Thermal diffusion in solid alloys. Acta Metallurgica **2**, 841–847 (1954)
8. Fast, J.D.: Interaction of Metals and Gases. Vol. 1. Macmillan (1965)

9. Fast, J.D.: Interaction of Metals and Gases. Vol. 2. Macmillan (1971)

10. Frost, H.J., Ashby, M.F.: Deformation-Mechanism Maps: The Plasticity and Creep of Metals and Ceramics. Pergamon Press, US (1982)

11. Gaude-Fugarolas, D.: Method for the reduction of interstitial elements in cast alloys and system for performing said method. Patent: US 8,286,692 B2. Awarded in US, China and Spain. Pending in Europe, and elsewhere.

12. Gaude-Fugarolas, D.: Modelling phase transformations on steel during induction hardening. In: International Conference on "Mathematical Modelling and Information Technologies in Welding and Related Processes" - Crimea (Ukraine) (2002)

13. Gaude-Fugarolas, D.: Modelling Induction Hardening. VDM Verlag Dr. Muller, Saarbrchen (2008). ISBN-10: 3639062965

14. Gaude-Fugarolas, D.: Hydrogen reduction during steel casting by thermally induced up-hill diffusion. In: Proceedings of METAL2010, Roznov pod Radhostem, Czech Republic. Tanger Ltd. (2010)

15. Gaude-Fugarolas, D.: Application of a physical model on interstitial diffusion to the issue of hydrogen damage during casting and forming of ferrous alloys. In: Proceedings of METAL2011, 18-20 May, Brno, Czech Republic. Tanger Ltd. (2011)

16. Gaude-Fugarolas, D.: Understanding hydrogen redistribution during steel casting, and its effective extraction by thermally induced up-hill diffusion. Journal of Iron and Steel Research International **18 supl.1.1**, 159–163 (2011)

17. Gaude-Fugarolas, D.: Effect of microstructure and trap typology on hydrogen redistribution in steel. In: Proceedings of METAL2013, Bnro, Czech Republic, 15-17 May 2013 (2013)

18. Gaude-Fugarolas, D.: On the effectiveness of baking as hydrogen embrittlement reduction treatment. In: Proceedings of METAL2014, 21-23 May, Brno, Czech Republic (2014)

19. Gaude-Fugarolas, D.: Prediction of hydrogen damage in steels. In: Proceedings of METAL2015, 3-5 June, Brno, Czech Republic (2015)

20. Hertzberg, R.W.: Deformation and fracture mechanics of engineering materials. John Wiley & sons, inc., New York (1996)

21. Hickel, T., McEniry, E.J., Nazarov, R., Leyson, G., Grabowski B. andNeugebauer, J.: Ab initio based understanding of the segregation and diffusion mechanisms of hydrogen in steels. In: Proceedings of SteelyHydrogen 2014, Ghent, Belgium, 5-7 May 2014, pp. 214–225 (2014)

22. Hirth, J.P.: Effects of hydrogen on the properties of iron and steel. Metallurgical Transactions A **11A**, 861–890 (1980)

23. Iino, M.: Evaluation of Hydrogen-Trap Binding Enthalpy I. Metallurgical Transactions A **18A**, 1559–1564 (1987)

24. Johnson, W.H.: On some remarkable change produced in iron and steel by the action of hydrogen and acids. Proceedings Royal Society London **23**, 168179 (1874)

25. Krom, A.H.M., Bakker, A.: Hydrogen trapping models in steel. Metallurgical and Materials Transactions B **31B**, 1475–1482 (2000)

26. Olden, V., Thaulow, C., Johnsen, R.: Modelling of hydrogen diffusion and hydrogen induced cracking in supermartensitic and duplex stainless steels. Materials and Design **29**, 1934–1948 (2008)

27. Poirier, D.R., Geiger, G.H.: Transport phenomena in materials processing. The Minerals, Metals & Materials Society, Warrendale (1994)

28. Rawdon, H.S.: Microstructural features of flaky steel. Transactions of the Metallurgical Society of AIME **62**, 246–286 (1919)

29. Takai, K., Chiba, Y., Noguchi, K., Nozue, A.: Visualization of the hydrogen desorption process from ferrite, pearlite, and graphite by secondary ion mass spectrometry. Metallurgical and Materials Transactions A **33A**, 2659–2665 (2002)

30. Turnbull, A., Hutchings, R., Ferriss, D.: Modelling of thermal desorption of hydrogen from metals. Materials Science and Engineering A **A238**, 317 328 (1997)

31. Zappfe, C.A., Sims, C.E.: Hydrogen embrittlement, internal stress and defects in steel. Transactions of the Metallurgical Society of AIME **145**, 225–271 (1941)